# Nikkomycin Biosynthesis: Formation of a 4-Electron Oxidation Product during Turnover of NikD with Its Physiological Substrate†

Robert C. Bruckner, Guohua Zhao, David Venci, and Marilyn Schuman Jorns*

*Department of Biochemistry, Drexel University, College of Medicine, Philadelphia, Pennsylvania 19102*

*Received April 1, 2004; Revised Manuscript Received May 6, 2004*

ABSTRACT: Nikkomycins are peptidyl nucleoside antibiotics that act as therapeutic antifungal agents in humans and easily degraded insecticides in agriculture. The nikkomycin peptidyl moiety contains a pyridyl residue derived from L-lysine. The first step in peptidyl biosynthesis is an aminotransferase-catalyzed reaction that converts L-lysine to $\Delta^1$- or $\Delta^2$-piperideine-2-carboxylate (P2C). Spectral, chromatographic, and kinetic analyses show that the aerobic reaction of nikD with P2C results in the stoichiometric formation of picolinate, accompanied by the reduction of 2 mol of oxygen to hydrogen peroxide. A high resolution HPLC method, capable of separating picolinate, nicotinate and isonicotinate, was developed and used in product identification. NikD contains 1 mol of covalently bound FAD and exists as a monomer in solution. Reductive and oxidative titrations with dithionite and potassium ferricyanide, respectively, show that FAD is the only redox-active group in nikD. Anaerobic reaction of nikD with 1 mol of P2C results in immediate reduction of enzyme-bound FAD. Because nikD is an obligate 2-electron acceptor, it is proposed that the observed 4-electron oxidation of P2C to picolinate occurs via a mechanism involving two successive nikD-catalyzed 2-electron oxidation steps. In addition to nikkomycins, a nikD-like reaction is implicated in the biosynthesis of an L-lysine-derived pyridyl moiety found in streptogramin group B antibiotics that are used as part of a last resort treatment for severe infections due to gram positive bacteria.

Nikkomycins are a closely related group of peptidyl nucleoside antibiotics that block the biosynthesis of chitin, the second most abundant polysaccharide in nature (after cellulose) (*1*−*3*). Chitin is important in maintaining the structural integrity of the cell walls of fungi and the exoskeleton of insects and other invertebrates. Chitin is not found in mammals. The dramatic increase in life-threatening fungal infections in immunocompromised patients has created a strong impetus for the development of new and safer antifugal drugs. Nikkomycins have proven effective as therapeutic antifungal agents in humans and as easily degraded insecticides in agriculture (*4*−*7*).

The first bacterial strain identified as a producer of nikkomycins (*Streptomyces tendae Tü901*) was isolated in 1970. The biosynthesis of nikkomycins is, however, only partially understood. The nucleoside and peptidyl moieties of nikkomycins are synthesized in separate pathways and then linked by a peptide bond (*8*). The biosynthesis of the peptidyl moiety is postulated to involve eleven enzymes, encoded by genes organized into two separate operons (*9, 10*). Only the first two enzymes in the pathway (nikC, nikD) have been isolated. The pyridyl residue and the attached carbon in the peptidyl moiety of nikkomycins originate from L-lysine (*9, 11*) (Scheme 1). The first step in peptidyl biosynthesis is catalyzed by nikC (*12*), an aminotransferase that converts L-lysine to the corresponding α-keto derivative. The α-keto derivative spontaneously cyclizes and dehydrates to yield $\Delta^1$- or $\Delta^2$-piperideine-2-carboxylate (P2C),[1] a compound that can exist in two tautomeric forms (*13*). The imine ($\Delta^1$-P2C) is the predominant tautomer at acid or neutral pH; the enamine ($\Delta^2$-P2C) is the major species at alkaline pH and is thought to be the more easily oxidized form (*14*).

Scheme 1: Postulated Role for NikD in the Biosynthesis of Nikkomycins[a]

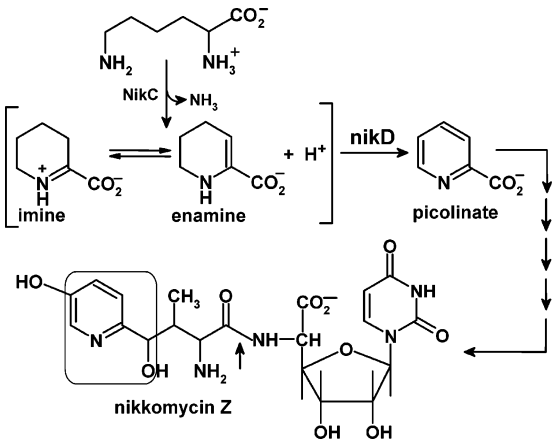


[a] An arrow shows the peptide bond that links the peptidyl and nucleosidyl portions of the antibiotic. Atoms derived from L-lysine are indicated by the box.

† This work was supported in part by Grant GM 31704 (M.S.J.) from the National Institutes of Health.

* To whom correspondence should be addressed. Tel.: (215) 762-7495 Fax: (215) 762-4452. E-mail: marilyn.jorns@drexel.edu.

[1] Abbreviations: P2C, $\Delta^1$- or $\Delta^2$-piperideine-2-carboxylate; $\Delta^1$-P2C, $\Delta^1$-piperideine-2-carboxylate; $\Delta^2$-P2C, $\Delta^2$-piperideine-2-carboxylate; DHP, dihydropicolinate; FAD, flavin adenine dinucleotide; EDTA, ethylenediaminetetraacetic acid; ESI-MS, electrospray ionization mass spectrometry; HEPES, *N*-2-hydroxyethylpiperazine-*N*′-2-ethanesulfonic acid.

10.1021/bi0493618 CCC: $27.50 
Published on Web 06/24/2004

The second step in peptidyl biosynthesis is catalyzed by nikD. Large amounts of the recombinant nikD have recently been isolated. The purified enzyme contains 1 mol of covalently bound FAD and catalyzes the oxidation of P2C, using oxygen as electron acceptor. In this reaction, oxygen was found to undergo a 2-electron reduction to hydrogen peroxide, but the P2C oxidation product was not identified (*15*). Nikkomycin synthesis in *S. tendae Tu901* is blocked by inactivation of the gene encoding nikD. Biosynthesis can be restored by adding picolinate (*9*), suggesting that nikD might catalyze an unusual 4-electron oxidation of P2C. In this paper, we present results consistent with this proposal and also show that nikD is an obligate 2-electron acceptor. The mechanistic consequences are discussed.

## EXPERIMENTAL PROCEDURES

*Materials.* Dried *Crotalus adamanteus* venom was obtained from Biotoxins, Inc. 3,4-Dehydro-L-proline, molecular weight standards and sodium dithionite were obtained from Sigma. $\epsilon$-*N*-Carbobenzoxy-L-lysine was purchased from Fluka.

*Enzyme Isolation and Steady-State Kinetics.* The recombinant form of nikD was purified as previously described (*15*). Steady-state kinetic studies were conducted in air-saturated buffer (100 mM potassium phosphate, pH 8.0) at 25 °C. Reactions were initiated by addition of nikD with an adder−mixer; spectral changes were recorded using an Agilent Technologies 8453 diode array spectrometer. Formation of hydrogen peroxide during turnover of nikD with P2C or 3,4-dehydro-L-proline was monitored using a horseradish peroxidase-coupled assay, as previously described (*16*). Turnover with P2C was also measured by monitoring formation of picolinate at 264 nm, using an extinction coefficient determined for the compound in 100 mM potassium phosphate buffer, pH 8.0 ($\epsilon_{264}$ = 3980 $M^{-1}$ $cm^{-1}$). Similarly, turnover with 3,4-dehydro-L-proline was measured by monitoring pyrrole-2-carboxylate formation at 256 nm ($\epsilon_{256}$ = 12 400 $M^{-1}$ $cm^{-1}$).

*Synthesis of P2C.* The imine isomer of P2C ($\Delta^1$-P2C) was prepared by a modification (*17*) of the method developed by Meister (*18*). Briefly, $\epsilon$-*N*-carbobenzoxy-L-lysine was oxidized to α-keto-$\epsilon$-*N*-carbobenzoxy-caproic acid using L-amino acid oxidase that was purified from dried *Crotalus adamanteus* snake venom (*19*, *20*). The carbobenzoxy group was removed from α-keto-$\epsilon$-*N*-carbobenzoxy-caproic acid with acetic acid-HBr, forming α-keto-$\epsilon$-amino-caproic acid as a transient intermediate that spontaneously cyclizes to yield the hydrobromide salt of P2C ($\Delta^1$-P2C), mp 188−189 °C, lit mp 190 °C (*17*). $FAB^+$ mass spectral analysis using a VG 70SE double focusing magnetic sector mass spectrometer yielded a prominent $MH^+$ peak at 128.0 amu, in agreement with the molecular weight calculated for the iminium cation of P2C ($C_6H_{10}NO_2^+$: 128.15). Stock solutions of P2C were prepared by dissolving the hydrobromide salt in water. An aliquot of each stock solution of P2C was diluted into 0.1 N NaOH. $\Delta^1$-P2C is converted to the enamine ($\Delta^2$-P2C) in 0.1 N NaOH (*13*). The concentration of P2C was estimated using the extinction coefficient reported for $\Delta^2$-P2C at 256 nm ($\epsilon_{256}$ = 725 $M^{-1}$ $cm^{-1}$) (*13*, *17*). The spectrophotometric estimate of P2C concentration was about 10% lower than that estimated based on weight.

*Chromatography and Spectroscopy.* HPLC analyses were conducted using a Rainin HPLC system equipped with a Hamilton PRP-X100 anion exchange column (10-$\mu$m, 4.6- × 250-mm). Isocratic elution was conducted at a flow rate of 1.4 mL/min at 25 °C. For method A, the elution solvent was prepared by mixing (v/v) 3 parts of a methanolic sodium carbonate solution (8.7 mM $Na_2CO_3$, 2.7 mM $NaHCO_3$ in 50% methanol (v/v)) with 1 part of acetonitrile. For method B, the elution solvent was prepared by mixing (v/v) 1 part of an aqueous sodium carbonate solution (17.4 mM $Na_2CO_3$, 5.2 mM $NaHCO_3$ in water) with 1 part of 50% methanol/water (v/v). The column eluate was monitored by its absorbance at 264 nm.

The molecular mass of nikD was estimated by size exclusion chromatography on a Sephadex G-150 column (1.5- × 72-cm) equilibrated with 20 mM HEPES buffer, pH 8.0, containing 150 mM NaCl and 1 mM EDTA at room temperature. The column was calibrated using molecular mass standards: carbonic anhydrase (29 kDa); bovine serum albumin (66 kDa); alcohol dehydrogenase (150 kDa); $\beta$-amylase (200 kDa). All runs were conducted at a flow rate of 0.2 mL/min, collecting 2.1-mL fractions.

Absorption spectra were recorded at 25 °C by use of an Agilent Technologies 8453 diode array spectrophotometer or a Perkin-Elmer Lambda 2S spectrometer. All spectra are corrected for dilution. The visible absorption spectrum of oxidized nikD is pH-dependent (*15*). Enzyme concentration was determined using extinction coefficients obtained for the absorption maximum at pH 8.0 ($\epsilon_{456}$ = 11 200 $M^{-1}$ $cm^{-1}$), pH 9.0 ($\epsilon_{458}$ = 10 430 $M^{-1}$ $cm^{-1}$) or pH 7.0 ($\epsilon_{455}$ = 12 380 $M^{-1}$ $cm^{-1}$). Anaerobic experiments were conducted using a special cuvette (*21*). Samples were made anaerobic by use of methods previously described (*21*). For reactions of nikD with P2C, substrate was tipped from a sidearm of the anaerobic cuvette. Stock solutions of sodium dithionite were made up in anaerobic 10 mM sodium borate buffer, pH 9.0, and standardized with riboflavin. The dithionite concentration was calculated as the average of results obtained in riboflavin titrations, conducted before and after titration of nikD. Photoreduction of nikD was conducted in 50 mM potassium phosphate buffer, pH 8.0, containing 120 mM EDTA and 1.0 $\mu$M 5-deazariboflavin, similar to that previously described (*15*). Stock solutions of potassium ferricyanide were prepared in anaerobic buffer (50 mM potassium phosphate, pH 8.0). The ferricyanide concentration was determined based on its absorbance at 420 nm ($\epsilon_{420}$ = 1040 $M^{-1}$ $cm^{-1}$). Titration results were corrected for the amount of ferricyanide required to oxidize photoreduced 5-deazariboflavin. In titration experiments, aliquots of dithionite or ferricyanide were added to the anaerobic cuvette (under positive argon pressure) using an argon-purged, gastight Hamilton syringe. Control titrations with ferricyanide were conducted with photoreduced *N*-methyltryptophan oxidase. The enzyme was purified and its concentration determined as previously described (*22*).

## RESULTS

*Identification of the Product Formed During Aerobic Turnover of NikD with P2C.* P2C exists mainly as the imine tautomer in acidic or neutral solution and exhibits only weak end absorption in the ultraviolet region (Figure 1, dashed curve). Addition of a catalytic amount of nikD to an aerobic

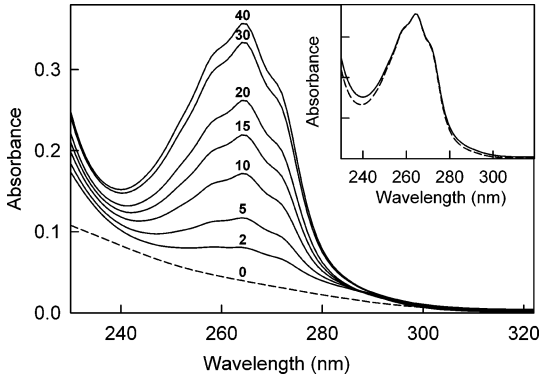


FIGURE 1: Aerobic reaction of nikD with P2C. The initial absorption spectrum of 85 $\mu$M P2C in 100 mM potassium phosphate buffer, pH 8.0, at 25 °C is shown by the dashed curve ($t$ = 0 min). The solid curves show absorption spectra recorded at various times ($t$ = 2, 5, 10, 15, 20, 30, and 40 min, respectively) after the addition of 150 nM nikD. The inset compares the absorption spectrum observed at the end of the reaction ($t$ = 40 min) with a spectrum (dashed line) recorded for solution containing 85 $\mu$M picolinate plus 150 nM nikD in the same buffer.

solution of P2C at pH 8 results in the time-dependent formation of a UV-absorbing species that exhibits a maximum at 264 nm (Figure 1, solid curves). The spectral properties of the oxidation product are virtually identical to that observed for an equimolar amount of picolinate (Figure 1, inset).

The spectral data suggested that the nikD reaction with P2C results in the quantitative conversion of P2C to picolinate. Further evidence was sought by using HPLC. A chromatographic method for the detection of picolinate in biological samples was recently reported that uses ion-pair chromatography on a C18 column (*23*). A broad peak was, however, observed for picolinate in preliminary studies using this method and the column was found to exhibit a very short half-life. Since picolinate exists as an anion at alkaline pH (p$K_1$ = 0.9; p$K_2$ = 5.0) (*24*), an alternate HPLC method was developed using an anion exchange column (Hamilton PRP-X100). A fairly sharp, symmetrical peak is observed for picolinate upon isocratic elution with sodium carbonate/methanol/acetonitrile (see method A in Experimental Procedures) (Figure 2, top trace). HPLC analysis was conducted using method A and aliquots withdrawn at various times after mixing nikD with P2C under aerobic conditions. As shown in Figure 2 (solid traces), the reaction of nikD with P2C was found to result in the time-dependent formation of a product exhibiting the same elution profile as picolinate. The amount of picolinate formed in the nikD reaction was estimated based on the area under the HPLC peak. The UV absorbance of same reaction mixture was also monitored continuously and used to estimate picolinate formation based on the increase of the absorbance at 264 nm. Excellent agreement was found between results obtained by both methods (Figure 3).

The qualitative and quantitative data presented in Figures 2 and 3 provide fairly compelling evidence that picolinate is produced from P2C in a nikD-dependent reaction. As will be discussed, the reaction of nikD with P2C is likely to involve a dihydropicolinate intermediate. None of the various possible isomers of dihydropicolinate are, however, known compounds. To compensate for the absence of a suitable dihydropicolinate standard, additional evidence to identify

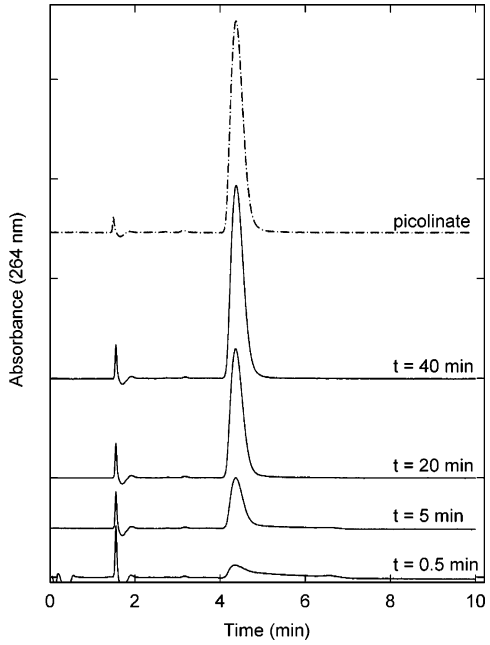


FIGURE 2: HPLC analysis of the progress of the aerobic reaction of nikD with P2C. Aliquots were withdrawn at the indicated times after mixing 150 nM nikD with 84.8 $\mu$M P2C in 50 mM potassium phosphate buffer, pH 8.0, at 25 °C, quenched by heating for 3 min at 100 °C and then cooled on ice. The samples were centrifuged prior to HPLC analysis using a PRP-X100 column and isocratic elution according to method A, as described in Experimental Procedures.

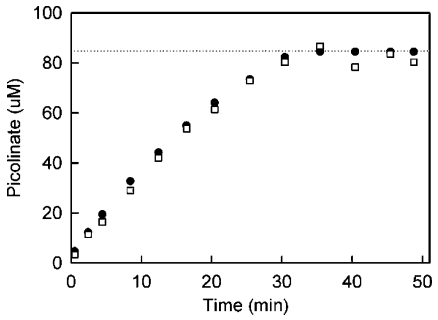


FIGURE 3: Comparison of the amount of picolinate detected in the reaction of nikD with P2C, as estimated by direct UV-absorbance measurements or quantitative HPLC analysis. The reaction of nikD with P2C was conducted as described in the legend to Figure 2. The filled circles show picolinate formation as estimated based on the increase in absorbance at 264 nm ($\epsilon_{264}$ = 3980 $M^{-1}$ $cm^{-1}$). Aliquots were withdrawn at various times from the same reaction mixture and subjected to HPLC analysis (method A). Picolinate was estimated by comparison of the area under the peak with a standard curve (open squares). The dotted line is the value expected for 100% conversion of P2C to picolinate.

picolinate was sought by developing a second HPLC method with enhanced resolution. Chromatography of picolinate on a PRP-X100 column appears to involve both anion exchange and hydrophobic interaction with the polymeric support of the column. Evidence for hydrophobic interaction is provided by the fact that elution time can be increased by decreasing the organic component in the elution solvent. In method B, isocratic elution is conducted using a more polar solvent (sodium carbonate in 25% methanol). This results in a 3-fold increase in picolinate elution time as compared with method A ($t$ = 14.3 vs 4.65 min). Importantly, significantly enhanced resolution is achieved with method B as judged by the observed baseline separation of picolinate and nicotinate ($t$

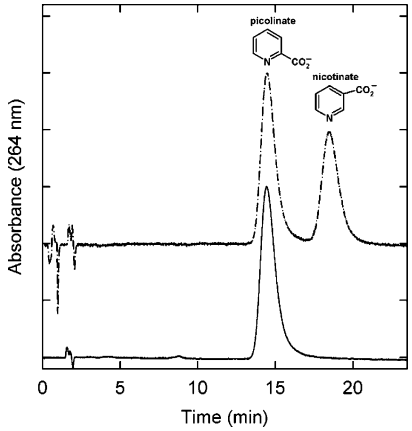


FIGURE 4: High-resolution HPLC analysis. NikD was reacted with P2C as described in the legend to Figure 2. After the reaction was complete (50 min), an aliquot was withdrawn, ultrafiltered, and subjected to HPLC analysis using method B, as described in Experimental Procedures (lower trace). The elution profile obtained for a standard mixture of picolinate and nicotinate is shown in the upper trace.

Table 1: Turnover of NikD with P2C[a]

| product measured | $k_{cat\ (app)}$ $min^{-1}$ | $K_{m\ (app)}$ ($\mu$M) |
|---|---|---|
| hydrogen peroxide | 72 ± 2 (64 ±2) | 2.9 ± 0.3 (5.2 ± 0.3) |
| picolinate | 37 ± 0.9 | 7.2 ± 0.6 |

[a] Apparent steady-state kinetic parameters were determined in air-saturated buffer as described in Experimental Procedures. Values in parentheses were taken from a previous publication (*15*).

= 14.3 vs 18.4 min), positional isomers where the carboxyl substituent is attached to adjacent carbons (C(2) and C(3), respectively) of the pyridine ring (Figure 4, top trace). (This method also separates these compounds from a third positional isomer, isonicotinate ($t$ = 14.9 min) (data not shown).) Using method B, the same elution profile is observed for picolinate and the product formed in the aerobic reaction of nikD with P2C (Figure 4, bottom trace).

*Kinetics of Picolinate Formation.* Picolinate formation is detected immediately upon mixing nikD with P2C in a stopped-flow spectrometer, as judged by the increase in absorbance at 264 nm with no evidence of an initial lag. Indeed, the initial rate is somewhat faster than the linear increase observed at $t$ > 4 s (Figure 5, panel A). Saturation kinetics are observed when the initial rate of picolinate formation is measured as a function of the concentration of P2C in air-saturated buffer (Figure 5, panel B). Saturation kinetics are also observed when the rate of P2C oxidation is measured by monitoring hydrogen peroxide formation using a horseradish peroxidase-coupled assay. The apparent $k_{cat}$ value obtained based on picolinate formation is 2-fold smaller than that obtained by monitoring hydrogen peroxide formation (Table 1). This difference is consistent with that expected for the 4-electron oxidation of P2C to picolinate, accompanied by the reduction of *two* molecules of oxygen to hydrogen peroxide.

Additional evidence in support of this conclusion was sought in control studies with 3,4-dehydro-L-proline, an alternate substrate for nikD that can only undergo a 2-electron oxidation to yield pyrrole-2-carboxylate (*15*) (eq 1). Similar values for apparent steady-state kinetic parameters are obtained with 3,4-dehydro-L-proline by monitoring hydrogen

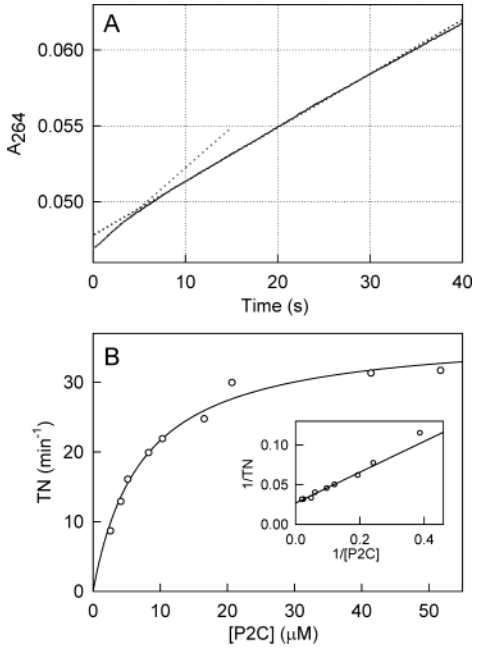


FIGURE 5: Kinetics of picolinate formation. Panel A shows the absorption increase at 264 nm observed immediately after mixing 200 nM nikD with 50 $\mu$M P2C, by use of a Hi-Tech Scientific stopped-flow spectrophotometer (SF-61DX2). The solid trace is the average of five shots conducted in 100 mM potassium phosphate buffer, pH 8.0 at 25 °C. The dotted lines are the linear regression fits to the data obtained at $t$ < 4 and > 4 s, respectively. Panel B is a plot of the rate of turnover of nikD as a function of the concentration of P2C. Turnover rates were measured in air-saturated buffer (100 mM potassium phosphate, pH 8.0) at 25 °C by monitoring the increase in absorbance at 264 nm due to picolinate formation ($\epsilon_{264}$ = 3980 $M^{-1}$ $cm^{-1}$), as detailed in Experimental Procedures. The inset to panel B shows the corresponding double reciprocal plot.

Table 2: Turnover of NikD with 3,4-Dehydro-L-proline[a]

| product measured | $k_{cat\ (app)}$ $min^{-1}$ | $K_{m\ (app)}$ (mM) |
|---|---|---|
| hydrogen peroxide | 18 ± 1 | 13 ± 2 |
| pyrrole-2-carboxylate | 19 ± 1 | 15 ± 2 |

[a] Apparent steady-state kinetic parameters were determined in air-saturated buffer, as described in Experimental Procedures. Hydrogen peroxide data were previously reported (*15*).

peroxide formation in a horseradish peroxidase-coupled assay or by measuring pyrrole-2-carboxylate formation at 256 nm in a direct spectrophotometric assay (Table 2).

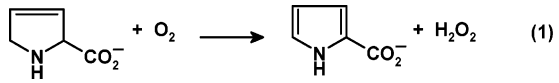


*Titration of NikD with Dithionite.* NikD contains 1 mol of covalently bound FAD (*15*), a prosthetic group that can accept a total of 2 electrons. Conversion of P2C to picolinate, however, involves a loss of 4 electrons. To determine whether nikD might contain a second redox-active group, reductive titration studies were conducted using dithionite, a potent 2-electron reductant. Anaerobic reduction of nikD with dithionite at pH 8.0 results in the isosbestic formation of a flavin radical intermediate (Figure 6, panel A), followed by an isosbestic conversion of the radical to fully reduced flavin (Figure 6, panel B). Radical formation is accompanied by a pronounced increase in absorption around 390 nm ($\lambda_{max}$ =

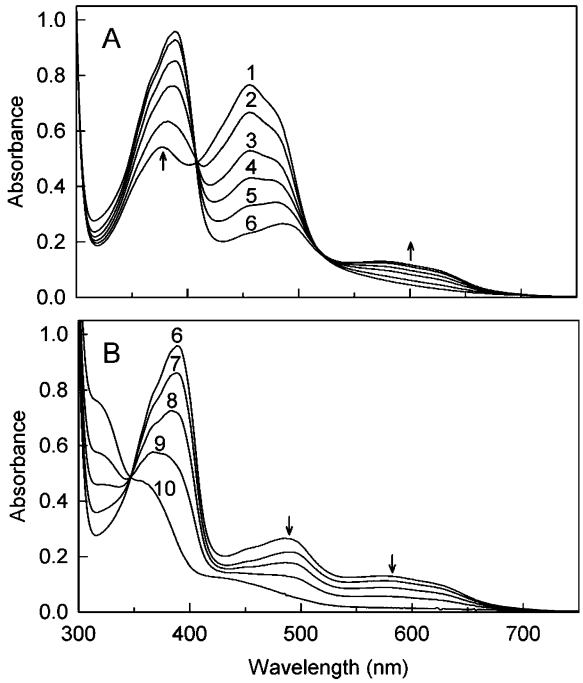


FIGURE 6: Reductive titration of oxidized nikD with dithionite. A sample of nikD (68.4 $\mu$M) in 1.0 mL of 100 mM potassium phosphate buffer, pH 8.0, at 25 °C was titrated with dithionite (337 $\mu$M) under anaerobic conditions. Arrows indicate the direction of spectral changes. Panel A shows the first phase of the titration. Curves 1−6 were recorded, after addition of 0, 20, 40, 60, 80, and 100 $\mu$L, respectively, of dithionite. Panel B shows the second phase of the titration. Curves 6−10 were recorded after addition of 100, 120, 140, 180, and 200 $\mu$L, respectively, of dithionite.

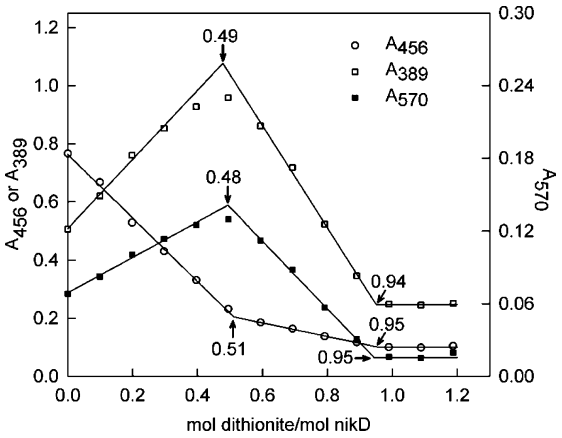


FIGURE 7: Stoichiometry of reduction of nikD with dithionite. Absorbance values observed at 456, 389, or 570 nm for the titration shown in Figure 6 are plotted versus mol dithionite/mol nikD.

389 nm), as expected for a red anionic flavin radical. This phase of the titration also results in a modest increase in absorption in the long wavelength region, a feature typically seen upon formation of a blue neutral radical. Maximal radical formation, as monitored at 389 or 570 nm, is observed upon addition of 0.5 mol of dithionite per mol of enzyme, whereas complete reduction of the enzyme requires 1.0 mol of dithionite (Figure 7). The same stoichiometry is observed for formation of maximal radical or fully reduced enzyme in dithionite titrations conducted at pH 9.0 or pH 7.0 (data not shown). Because two electrons are required to convert oxidized flavin to the fully reduced form, the results strongly suggest that the covalent FAD is the only redox-active group in nikD.

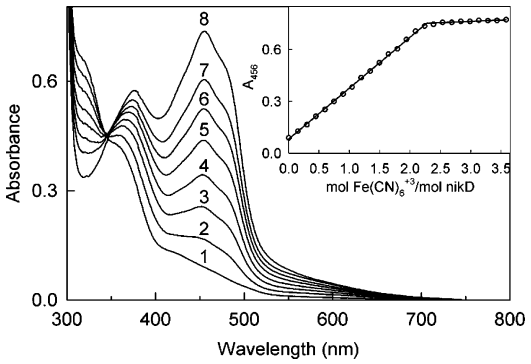


FIGURE 8: Oxidative titration of photoreduced nikD with potassium ferricyanide. The reduced enzyme (curve 1) was prepared by irradiating an anaerobic solution of nikD (68.6 $\mu$M) in 1.0 mL of 50 mM potassium phosphate buffer, pH 8.0, containing 120 mM EDTA and 1.0 $\mu$M 5-deazariboflavin, as previously described (*15*). Curves 2−8 were recorded after addition of 40, 80, 120, 160, 200, 240, and 300 $\mu$L, respectively, of an anaerobic solution of potassium ferricyanide (511.7 $\mu$M). The inset shows a plot of absorbance at 456 nm as a function of mol potassium ferricyanide/mol nikD.

*Oxidative Titration of Photoreduced NikD with Ferricyanide.* Additional evidence was sought by oxidative titration of photochemically reduced enzyme with potassium ferricyanide, a potent 1-electron oxidant. Photoreduction of nikD at pH 8.0 proceeds via the isosbestic formation of a radical intermediate with spectral properties identical to those observed with dithionite at this pH. Further irradiation converts the radical to fully reduced flavin, as observed with dithionite (*15*). Interestingly, a radical intermediate is not observed during reoxidation of the photoreduced enzyme with ferricyanide. Instead, titration with ferricyanide yields oxidized enzyme in a nearly isosbestic reaction that is complete upon addition of slightly more than 2 equivalents of ferricyanide (2.27 $K_3Fe(CN)_6$/mol enzyme) (Figure 8). Control studies were conducted with *N*-methyltryptophan oxidase, a flavoenzyme known to contain 1 mol of covalently bound FAD as its only redox-active group (*22*, *25*). Reoxidation of photoreduced *N*-methyltryptophan oxidase was also found to require slightly more than 2 equiv of ferricyanide (2.28 mol $K_3Fe(CN)_6$/mol enzyme). The oxidative titration results provide further evidence that FAD is the only redox-active group in nikD.

*Gel Filtration Studies.* A molecular mass of 44 904 Da is calculated for nikD apoenzyme plus FAD, a value that agrees with results obtained by ESI-MS analysis (*15*). Formation of a functional dimer in solution might enable nikD to act as a 4-electron acceptor. A molecular mass of 47.7 kDa for nikD was estimated by size exclusion chromatrography on Sephadex G-150. The gel filtration studies show that nikD exists as a monomer in solution. These results, in conjunction with those obtained in redox titrations, provide compelling evidence that nikD is an obligate 2-electron acceptor.

*Anaerobic Reaction of NikD with 1.0 or 0.5 mol of P2C.* Anaerobic reaction of nikD with *1 mol* of P2C results in the immediate reduction of enzyme-bound FAD. The absorption spectrum of substrate-reduced enzyme is virtually identical to that observed upon reduction with 1 mol of dithionite (Figure 9A). Anaerobic reaction of nikD with *0.5 mol* of P2C results in the immediate loss of 50% of the flavin absorbance at 456 nm, followed by further reduction in a slow reaction to yield a species with spectral properties

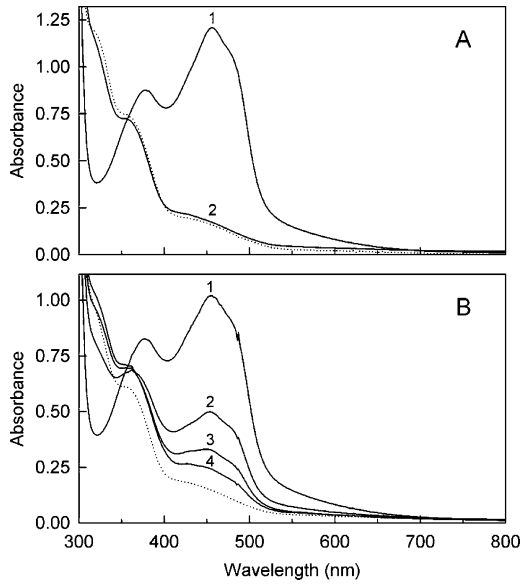


FIGURE 9: Reduction of nikD with P2C. Reactions were conducted under anaerobic conditions in 100 mM potassium phosphate buffer, pH 8.0, at 25 °C. (A) The solid lines show absorption spectra recorded before (curve 1) and immediately after (curve 2) mixing nikD (108 $\mu$M) with an equimolar amount of P2C. The dotted line is the absorption spectrum of dithionite-reduced nikD (108 $\mu$M), calculated using the data in Figure 6B, curve 10. (B) Absorption spectra of nikD (91.1 $\mu$M) were recorded before (curve 1) and immediately after (curve 2) addition of 47 $\mu$M P2C. Curves 3 and 4 were recorded at 1.5 and 18 h, respectively, after P2C addition. The dotted line is the absorption spectrum of fully reduced nikD (91.1 $\mu$M), calculated using the data in Panel A, curve 2.

similar to that observed immediately after reaction with 1 mol of P2C (Figure 9B).

## DISCUSSION

Qualitative and quantitative analyses, using spectral and chromatographic methods, demonstrate that the aerobic reaction of nikD with its physiological substrate results in the stoichiometric conversion to picolinate. This 4-electron oxidation reaction is accompanied by the reduction of two mol of oxygen to hydrogen peroxide. The results are consistent with earlier microbiological studies that show that nikkomycin biosynthesis with a mutant strain of *S. tendae Tu901* lacking nikD can be restored by adding picolinate to the growth medium (*9*). Other studies provide definitive evidence that nikD is an obligate 2-electron acceptor. First, complete reduction of the enzyme requires one mol of dithionite, a potent 2-electron reductant. Complete reoxidation of photoreduced nikD is achieved with 2 mol of potassium ferricyanide, a strong 1-electron oxidant. Gel filtration studies show that nikD exists as a monomer in solution. Finally, recent crystallographic data show that nikD crystals contain one molecule in the asymmetric unit and that FAD is the only redox center at the enzyme active site.[2]

Given that nikD can accept only two electrons at a time, the observed 4-electron oxidation of P2C to picolinate would appear to necessitate a mechanism involving two successive nikD-catalyzed 2-electron oxidation steps (Scheme 2). The initial 2-electron oxidation step converts P2C to a dihydropicolinate (DHP) intermediate. This step is observed upon anaerobic reaction of nikD with 1 mol of P2C, as judged by the immediate conversion of oxidized enzyme to the fully reduced state. Reoxidation of the reduced enzyme by reaction with oxygen occurs under aerobic conditions and enables a second 2-electron oxidation step that converts DHP to picolinate. According to the mechanism in Scheme 2, the 4-electron oxidation of P2C proceeds without dissociation of the DHP intermediate. Excess substrate inhibition is not observed when picolinate formation is monitored in air-saturated buffer at P2C concentrations 7-fold greater than the apparent $K_m$. This suggests that the labile DHP intermediate is not released into solution, because excess substrate inhibition would be expected if DHP must compete with P2C in binding to oxidized enzyme.

Anaerobic reaction of nikD with 0.5 mol of P2C results in the immediate reduction of 50% of the enzyme flavin, followed by further reduction in a slow reaction. The fast phase is attributed to conversion of half of the enzyme to a reduced enzyme complex with DHP ($EFADH_2$−DHP). Several mechanisms that might account for the slow reduction phase are outlined in Scheme 3. In mechanism A, $EFADH_2$−DHP is reoxidized in a slow reaction with oxidized nikD to yield a redox-competent complex ($EFAD_{ox}$−DHP) identical with a postulated intermediate in the normal catalytic reaction (see Scheme 2). In mechanism B, slow dissociation of the $EFADH_2$−DHP complex releases DHP into solution. DHP re-binds to oxidized enzyme to yield the same redox-competent complex ($EFAD_{ox}$−DHP) as in mechanism A. Mechanism C is also initiated by slow dissociation of the $EFADH_2$−DHP complex but differs from mechanism B with respect to the fate of the released DHP. In mechanism C, 2 molecules of DHP are converted to 1 each of picolinate and P2C. The P2C formed in this nonenzymic disproportionation reaction will, of course, react rapidly with oxidized enzyme.

The 4-electron oxidation reaction postulated for nikD in Scheme 2 resembles reactions observed with choline oxidase and thiamine oxidase, enzymes that contain a single covalently bound flavin as the only redox-active group. Choline

Scheme 2: Proposed Mechanism for the NikD-Catalyzed Oxidation of P2C to Picolinate (P)

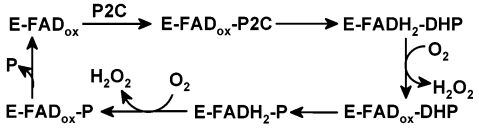


Scheme 3: Possible Mechanisms for the Slow, Second Phase of NikD Reduction Observed during Anaerobic Reaction of the Enzyme with 0.5 mol of P2C

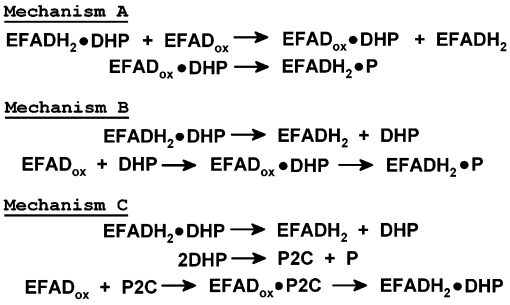


[2] Carrell, C. J., Venci, D., Bruckner, R. C., Jorns, M. S., Mathews, F. S., unpublished results.

Scheme 4: Representative Structure of a Streptogramin Group B Antibiotic[a]

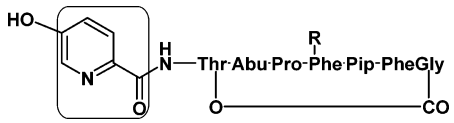


[a] A box indicates atoms derived from L-lysine. Abu, α-aminobutyric acid; Pip, pipecolic acid; PheGly, phenylglycine.

oxidase and thiamine oxidase catalyze the 4-electron oxidation of alcohol substrates to the corresponding carboxylic acids via two successive 2-electron oxidation steps, a mechanism analogous to that postulated for the nikD reaction (*26*−*28*). The successive 2-electron oxidation steps in the choline and thiamine oxidase reactions, however, occur at the *same* carbon atom and may be chemically equivalent if the aldehyde intermediate is hydrated prior to the second oxidation step. In contrast, the two successive oxidation steps in the nikD reaction would appear to involve *different* atoms and may be chemically nonequivalent (i.e., C−N versus C−C bond oxidation).

The results presented in this study demonstrate that a quantitative 4-electron oxidation of P2C to picolinate occurs in a nikD-*dependent* reaction. The data are compatible with two successive, nikD-catalyzed 2-electron oxidation steps, as proposed in Scheme 2. The various isomers of DHP are likely to be unstable, and none are known compounds. Therefore, we cannot definitively rule out the possibility that picolinate might be formed in a nonenzymic reaction, such as disproportionation or oxidation of the free DHP intermediate. It is, however, important to note that the initial nikD-catalyzed oxidation of P2C to DHP must be rate-determining in the overall 4-electron oxidation of P2C, as judged by the observed rates of hydrogen peroxide and picolinate formation (see Table 1). Also, picolinate formation is observed immediately after mixing nikD with P2C with no evidence of an initial lag phase. A fast, nonenzymic disproportionation of DHP appears unlikely, as judged by the slow disproportionation reaction observed with a dihydropryidinium compound that produces a more a highly conjugated product as compared with picolinate (*29*, *30*). Nonenzymic oxidation of a 2,3-dehydroproline derivative to the corresponding aromatic pyrrole has been postulated as a step in the biosynthesis of coumermycin $A_1$ and pyoluteorin antibiotics (*31*, *32*) but no information is available regarding the rate of the nonenzymic reaction.

The mechanism proposed in Scheme 1 for the biosynthesis of the pyridyl ring in nikkomycins may be relevant to the biosynthesis of a similar moiety found in streptogramin group B antibiotics (Scheme 4). Streptogramins are potent antibacterial agents that use the synergistic action of streptogramins A and B to inhibit bacterial protein synthesis. A streptogramin pair, Synercid, has recently been approved as a last resort treatment for severe infections due to gram positive bacteria, such as methicillin-resistant *Staphylococcus aureus* and vancomycin-resistant *Enterococcus faecium* (*33*). The pyridyl moiety in group B streptogramins is derived from L-lysine and essential for antibacterial activity (*33*). Its mode of biosynthesis is not fully understood but is known to involve an L-lysine-2-aminotransferase like nikC in the nikkomycin pathway (*34*−*36*), suggesting that the streptogramin pathway will also involve a P2C oxidase similar to nikD.

## ACKNOWLEDGMENT

We thank Jeffrey Horovich for performing mass spectral analyses.

## REFERENCES

1. Brillinger, G. U. (1979) Metabolic products of microorganisms. 181. Chitin synthetase from fungi, a test model for substances with insecticidal properties, *Arch. Microbiol. 121*, 71−74.
2. Dahn, U., Hagenmaier, H., Hohne, H., Konig, W. A., Wolf, G., and Zahner, H. (1976) Stoffwechselprodukte von mikroorganismen. 154. Mitteilung. Nikkomycin ein neuer hemmstoff der chitin-synthese bein pilzen, *Arch. Microbiol. 107*, 143−160.
3. Fiedler, H.-P., Kurth, R., Langharig, J., Delzer, J., and Zahner, H. (1982) Nikkomycins: Microbial inhibitors of chitin synthetase, *J. Chem. Biotechnol. 32*, 271−280.
4. Hector, R. F., Zimmer, B. L., and Pappagianis, D. (1990) Evaluation of nikkomycins X and Z in murine models of coccidioidomycosis, *Antimicrob. Agents Chemother. 34*, 587−593.
5. Hector, R. F. and Schaller, K. (1992) Positive interaction of nikkomycins and azoles against *Candida albicans* in vitro and in vivo, *Antimicrob. Agents Chemother. 36*, 1284−1289.
6. Zhang, D. and Miller, M. J. (1999) Polyoxins and nikkomycins: progress in synthetic and biological studies, *Curr. Pharm. Des. 5*, 73−99.
7. Hector, R. F. (1993) Compounds active against cell walls of medically important fungi, *Clin. Microb. Rev. 6*, 1−21.
8. Bormann, C., Mattern, S., Schrempf, H., Fiedler, H. P., and Zahner, H. (1989) Isolation of *Streptomyces tendae* mutants with an altered nikkomycin spectrum, *J. Antibiot. 42*, 913−918.
9. Bruntner, C., Lauer, B., Schwarz, W., Mohrle, V., and Bormann, C. (1999) Molecular characterization of co-transcribed genes from *Streptomyces tendae Tu901* involved in the biosynthesis of the peptidyl moiety of the peptidyl nucleoside antibiotic nikkomycin, *Mol. Gen. Genet. 262*, 102−114.
10. Lauer, B., Russwurm, R., Schwarz, W., Kalmanczhelyi, A., Bruntner, C., Rosemeier, A., and Bormann, C. (2001) Molecular characterization of co-transcribed genes from *Streptomyces tendae Tu901* involved in the biosynthesis of the peptidyl moiety and assembly of the peptidyl nucleoside antibiotic nikkomycin, *Mol. Gen. Genet. 264*, 662−673.
11. Sommer, U. (1983) Untersuchungen zur biosynthese von nikkomycin D, Ph.D. Thesis, Universität Munster.
12. Bruntner, C. and Bormann, C. (1998) The *Streptomyces tendae Tu901* L-lysine 2-aminotransferase catalyzes the initial reaction in nikkomycin D biosynthesis, *Eur. J. Biochem. 254*, 347−355.
13. Macholan, L. and Svatek, E. (1960) Aminoketocarbonsauren VL: Über die konstitution and strukturformen der α-keto-analoga natürlichler diaminosäuren, *Collection Czechoslov. Chem. Commun. 25*, 2564−2575.
14. Nishina, Y., Sato, K., and Shiga, K. (1991) Isomerization of Δ-1-piperideine-2-carboxylate to Δ-2-piperideine-2-carboxylate on complexation with the flavoprotein D-amino acid oxidase, *J. Biochem. 109*, 705−710.
15. Venci, D., Zhao, G., and Jorns, M. S. (2002) Molecular characterization of nikD, a new flavoenzyme important in the biosynthesis of nikkomycin antibiotics, *Biochemistry 41*, 15795−15802.
16. Wagner, M. A. and Jorns, M. S. (2000) Monomeric sarcosine oxidase: 2. Kinetic studies with sarcosine, alternate substrates and substrate analogues, *Biochemistry 39*, 8825−8829.
17. Roseman, M. A. (1970) A model system analysis of the mechanism of 2-keto-3-deoxy-6-phosphogluconic acid aldolase: The role of the Schiff base intermediate, Ph.D. Thesis, Michigan State University.
18. Meister, A. (1954) The α-keto analogues of arginine, ornithine and lysine, *J. Biol. Chem. 206*, 577−585.
19. Wellner, D. and Meister, A. (1960) Crystalline L-amino acid oxidase of *Crotalus adamanteus*, *J. Biol. Chem. 235*, 2013−2018.
20. Raibekas, A. A. and Massey, V. (1997) Glycerol-assisted restorative adjustment of flavoenzyme conformation perturbed by site-directed mutagenesis, *J. Biol. Chem. 272*, 22248−22252.

21. Wagner, M. A., Trickey, P., Chen, Z., Mathews, F. S., and Jorns, M. S. (2000) Monomeric sarcosine oxidase: 1. Flavin reactivity and active site binding determinants, *Biochemistry 39*, 8813−8824.
22. Wagner, M. A., Khanna, P., and Jorns, M. S. (1999) Structure of the flavocoenzyme of two homologous amine oxidases: Monomeric sarcosine oxidase and *N*-methyltryptophan oxidase, *Biochemistry 38*, 5588−5595.
23. Dazzi, C., Candioano, G., Massazza, S., Ponzetto, A., and Varesio, L. (2001) New high-performance liquid chromatographic method for the detection of picolinic acid in biological fluids, *J. Chromatogr. B 751*, 61−68.
24. Garcia, B., Ibeas, S., and Leal, J. M. (1996) Zwitterionic pyridenecarboxylic acids, *J. Phys. Org. Chem. 9*, 593−597.
25. Khanna, P. and Jorns, M. S. (2001) Characterization of the FAD-containing *N*-methyltryptophan oxidase from *Escherichia coli*, *Biochemistry 40*, 1441−1450.
26. Gomez-Moreno, C., Choy, M., and Edmondson, D. E. (1979) Purification and properties of the bacterial flavoprotein: Thiamin dehydrogenase, *J. Biol. Chem. 254*, 7630−7635.
27. Gomez-Moreno, C. and Edmondson, D. E. (1985) Evidence for an aldehyde intermediate in the catalytic mechanism of thiamine oxidase, *Arch. Biochem. Biophys. 239*, 46−52.
28. Gadda, G. (2002) Mechanistic studies on choline oxidase from *Arthrobacter globiformis*, in *Flavins and Flavoproteins 2002* (Chapman, S., Perham, R., and Scrutton, N., Eds.) pp 181−186, Rudolf Weber, Berlin.
29. Chiba, K., Peterson, L. A., Castagnoli, K. P., Trevor, A. J., and Castagnoli, N. (1985) Studies on the molecular mechanism of bioactivation of the selective nigrostriatal toxin 1-methyl-4-phenyl-1,2,3,6-tetrahydropyridine, *Drug Metab. D. 13*, 342−347.
30. Castagnoli, N., Chiba, K., and Trevor, A. J. (1985) Potential bioactivation pathways for the neurotoxin 1-methyl-4-phenyl-1,2,3,6-tetrahydropyridine (MPTP), *Life Sci. 36*, 225−230.
31. Thomas, M. G., Burkart, M. D., and Walsh, C. T. (2002) Conversion of L-proline to pyrrolyl-2-carboxyl-S−PCP during undecylprodigiosin and pyoluteorin biosynthesis, *Chem. Biol. 9*, 171−184.
32. Wang, Z., Li, S., and Heide, L. (2000) Identification of the coumermycin $A_1$ biosynthetic gene cluster of *Streptomyces rishiriensis* DSM 40490, *Antimicrob. Agents Chemother. 44*, 3040−3048.
33. Barriere, J. C., Berthaud, N., Beyer, D., Dutka-Malen, S., Paris, J. M., and Desnottes, J. F. (1998) Recent developments in streptogramin research, *Curr. Pharm. Des. 4*, 155−180.
34. Reed, J. W., Purvis, M. B., Kingston, D. G. I., Biot, A., and Gossele, F. (1989) Biosynthesis of antibiotics of the Virginiamycin family. 7. Stereo- and regiochemical studies on the formation of the 3-hydroxypicolinic acid and pipecolic acid units, *J. Org. Chem. 54*, 1161−1165.
35. Blanc, V., Thibaut, D., Bamas-Jacques, N., Blanche, F., Crouzet, J., Barriere, J. C., Debussche, L., Famechon, A., Paris, J. M., and Dutruc-Rosset, G. (2002) Streptogramins for preparing same by mutasynthesis, US Patent 6,352,839 B1.
36. Namwat, W., Kinoshita, H., and Nihira, T. (2002) Identification by heterologous expression and gene disruption of *visA* as L-lysine 2-aminotranferse essential for virginiamycin S biosynthesis in *Streptomyces virginiae*, *J. Bacteriol. 184*, 4811−4818.

BI0493618